Cement and Concrete Research 40 (2010) 1393–1402

Contents lists available at ScienceDirect

Cement and Concrete Research

journal homepage: http://ees.elsevier.com/CEMCON/default.asp

Measurement and simulation of dendritic growth of ice in cement paste

Zhenhua Sun, George W. Scherer *

Civil & Env. Eng., Princeton University, Princeton, NJ 08544 USA

ARTICLE INFO

Article history:
Received 30 November 2009
Accepted 15 March 2010

Keywords:
Pore size distribution (B)
Durability (C)
Freezing and thawing (C)
Modeling (E)

ABSTRACT

We re-examine experiments by Helmuth (1962) from which he concluded that ice grows in the pores of cement paste under heat-flow control, and that the internal temperature rises to the melting point given by the Gibbs–Thomson equation. We find that his conclusions are correct, but the growth rates he reports are misleading. Using experimental and computational methods, we show that the ice grows in the form of dendrites, which allows a constant growth rate under heat-flow control. A modification of the experimental procedure permits accurate measurement of the growth rate of ice in the pores.

1. Introduction

Frost damage is one of the main reasons for deterioration of concrete infrastructure in cold regions, so many studies have been conducted to understand the damage mechanism [1]. Powers [2] proposed that the cause of damage is the hydraulic pressure that results from the volume expansion when water freezes. However, experiments later cast doubt on this idea. For example, Beaudoin and MacInnis [3] measured the length change of concrete during freezing after the pore water had been exchanged with benzene. From the fact that the concrete still expanded, even though the volume of benzene decreases during freezing, they suggested that crystallization pressure is the true reason for frost damage. Recent study in our lab [4] shows that the hydraulic and crystallization pressures are both capable of doing damage to concrete, and one may be dominant over the other under different conditions.

One of the most successful methods for protecting concrete from frost damage is to introduce air voids into concrete. Powers [2] argued that the air voids offer room into which water can expand when it freezes, thereby releasing the hydraulic pressure. This also proved to be an inadequate explanation, as Powers and Helmuth later demonstrated that concrete with air voids does not simply stop expanding, but actually shrinks during freezing [5]. This shrinkage is caused by the cryo-suction mechanism, which is described below.

The solution in the pores of cement paste (typically, ~0.5 M alkali hydroxide [6]) will not freeze at the normal melting point, because of the curvature, κ_{CL}, imposed on the ice crystals by the pore wall. The melting point decreases as the pore becomes smaller according to the Gibbs–Thomson equation [7], which can be expressed by [8]:

$$T_m(\kappa_{CL}) = T_m(0) - \frac{\gamma_{CL}\kappa_{CL}}{\Delta S_{fv}} \quad (1)$$

where $T_m(0)$ is the melting point of a flat macroscopic crystal, γ_{CL} is the crystal/liquid interfacial energy, and ΔS_{fv} is the entropy of fusion per unit volume of crystal; for ice, $\Delta S_{fv} \approx 1.2$ J/(cm^3 K). In a cylindrical pore, the tip of the advancing crystal can be approximated as hemispherical, so the curvature is

$$\kappa_{CL} = \frac{2}{r_p - \delta} \quad (2)$$

where δ is the thickness of the unfrozen layer of liquid against the pore wall. For water, δ is normally on the order of ~0.8 nm [9]; in cement paste, $\delta \approx 1.0$–1.2 nm [10]. The mesopores[1] in concrete are much smaller than the air voids (*viz.*, tens of nanometers for mesopores versus tens of microns for the voids), so the melting point in mesopores is much lower. Consequently, ice will stay in the air voids without entering the mesopores until the temperature is low enough to satisfy Eq. (1). While trapped in the voids, the macroscopic ice tends to suck water from the mesopores to the voids (*i.e.*, exerts "cryo-suction"), which generates a negative pressure on the concrete body and causes the shrinkage [4,5,8,11].

Decades of work, summarized in several reviews [1,8,12], have greatly enhanced our understanding of frost damage. However, there are still issues left unaddressed, such as how the ice nucleates, and its rate and pattern of growth. These questions are important for the

* Corresponding author. Eng. Quad. E-319, Princeton University, Princeton, NJ 08544 USA.
E-mail address: scherer@princeton.edu (G.W. Scherer).

[1] According to IUPAC, a mesopore has a diameter between 2 and 50 nm.

0008-8846/$ – see front matter © 2010 Elsevier Ltd. All rights reserved.
doi:10.1016/j.cemconres.2010.03.008

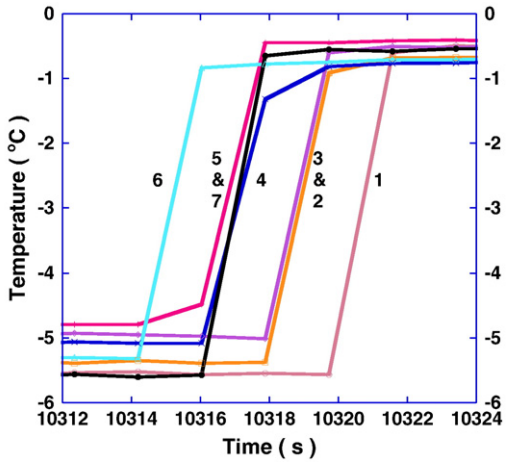

Fig. 1. Sequential temperature change in a line of 7 thermocouples spaced about 25 mm apart as ice propagates through the cement paste [data from Kumpf, ref. [14]]. The sample was equilibrated at about −5 °C in a kerosene bath; nucleation occurred spontaneously near thermocouple 6, then reached 5 and 7 almost simultaneously. The temperature jumps do not occur at equal time intervals as the ice passes thermocouples 6–5–4–3–2–1. The final temperature after the jump is about −0.7 °C.

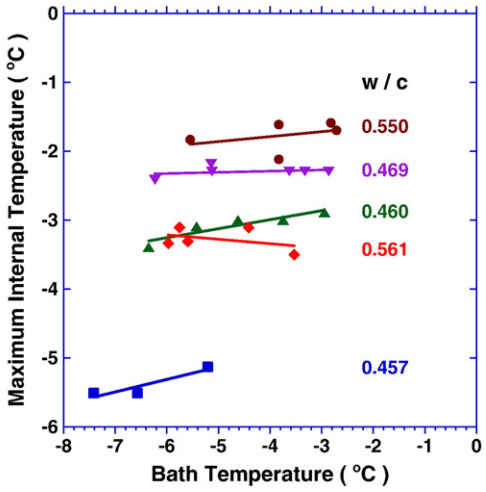

Fig. 2. The final temperatures measured by Helmuth [13] as the ice passed his thermocouples were roughly constant for a given type of paste, independent of the temperature of the surrounding bath. Data from ref. [13].

analysis of freezing stresses, the development of a more detailed understanding of the source of damage, and development of better ways to protect concrete. The goal of the current study is to explore these topics.

Helmuth [13] conducted highly illuminating experiments to study ice growth in cement paste. He cut blocks of paste into rectangular prisms and embedded thermocouples along the length of the samples, which were then cooled down in a kerosene bath to temperatures near −5 °C. Some of the samples froze from spontaneous (heterogeneous) nucleation, while the others were touched with a piece of ice to initiate the crystallization. As ice propagates through the sample, heat is released. By monitoring the temperature change of the thermocouples, Helmuth was able to get information about the ice growth rate. Similar experiments were performed by Kumpf [14,15] to verify some of Helmuth's conclusions. The experiments from both authors yielded similar results, as described in detail below. Helmuth noticed that the thermocouples jumped to a higher temperature sequentially as ice propagated from the nucleation site throughout the sample (Fig. 1). More importantly, he found that the final temperatures of the thermocouples were rather consistent for a certain type of cement sample, no matter what the external bath temperature was (Fig. 2). Helmuth argued that the final temperature is the melting point of water in the pores of the cement paste sample (usually <0 °C due to the Gibbs–Thomson effect). When water freezes, the latent heat increases the temperature of the sample. As the temperature approaches the melting point, the ice growth rate slows down, and becomes controlled by the rate at which the heat is transferred away. The implication of the temperatures measured inside the samples is that ice growth in cement paste is heat-flow controlled. Another finding from the experiment was the ice growth rate. As both the positions of thermocouples and the time when ice passes by are known, the growth rate of ice can be easily calculated (Fig. 3). Both Helmuth and Kumpf's experiments showed that the ice growth rate was roughly 1–3 cm/s for bath temperatures in the range of −1 to −8 °C.

Helmuth's results and interpretation sound plausible, until we notice that the growth rates found from these experiments are comparable to results from Hillig and Turnbull [16] (H–T), in which they studied ice growth in a capillary tube. In their experiments, the latent heat during freezing was transferred away rapidly through the capillary tube wall, so the ice grew freely without being slowed down by the heat accumulation. The growth rate was controlled by the rate at which water molecules could attach to the ice/water interface at a given undercooling. This is the fastest growth rate that ice can achieve, which was found from their experiments to be about

$$u(\mathrm{cm/s}) = 0.16(T_m - T)^{1.7} \tag{3}$$

where u is the grow rate in cm/s, T is the water temperature and T_m is the melting point (both in °C). For water in the small pores, T_m is determined by Eq. (1). Questions have been raised as to whether the growth rates measured by H–T were actually controlled by heat flow [17]. To investigate this question, in Fig. 4, we compare their measurements to the theoretical expression for the rate of growth of dendrites of ice under heat-flow control [18,19]. This theory was shown to describe very accurately a large body of experimental data assembled by Shibkov et al. [20] for the growth of ice under conditions of heat-flow control; at the highest undercoolings, the theory slightly over-estimated the rate of dendritic growth. However, the data of H–T lie well above the theoretical curve, which indicates that the rates they measured were not controlled by heat flow, particularly for smaller undercoolings. On the contrary, from the temperature dependence represented by Eq. (3), H–T concluded that the rate of growth was controlled by the rate of attachment of molecules to a screw dislocation in the surface of the ice crystal [16]. As shown in

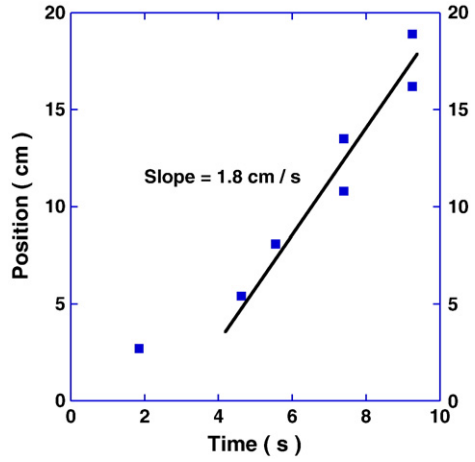

Fig. 3. Ice growth rate indicated by temperature change of thermocouples as shown in Fig. 1 [data from Kumpf, ref. [14]].

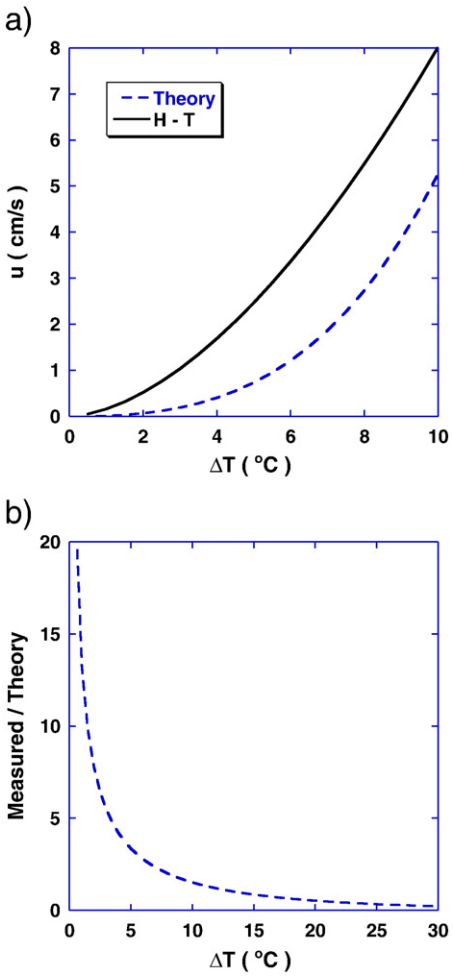

Fig. 4. (a) Data of Hillig and Turnbull [16] for the growth rate of ice, u, versus undercooling, $\Delta T = T_m - T$ (H–T, solid curve) compared with the theory of Langer and Müller-Krumbarr [18] (Theory, dashed curve) using properties from Shibkov et al. [20]; (b) ratio of curves from part (a) showing convergence at large undercoolings.

Fig. 4b, as the undercooling increases, the curves tend to converge, which suggests that heat flow began to influence the measurements as the growth rate increased. We conclude that, for the range of undercoolings explored in our experiments, the intrinsic (interface-controlled) growth rate can be represented by Eq. (3).

The question then becomes, how can the growth rate found by Helmuth, which seemed to be controlled by heat flow, be comparable to the free ice growth rate found by Hillig and Turnbull? To investigate these contradictory findings, we decided to extend Helmuth's study both numerically and experimentally.

2. Numerical simulation

2.1. Level set method

The goal of the simulation is to show the growth rate and morphology of ice as it propagates in supercooled cement paste. As was shown in Hillig and Turnbull's work, the ice growth rate is directly related to the interface temperature through Eq. (3). As the ice grows, it releases the heat of fusion, ΔH_f (J/mole), which increases the temperature of the sample, and slows down the growth. The final growth rate will thus depend not only on the degree of initial supercooling, but also on the rate at which the generated heat is transferred away, which depends on the shape of the ice front and the temperature gradient in that region. By solving for the heat transfer and ice propagation rates iteratively, we are able to track the water/ice interface.

The governing equation for heat transfer is

$$\rho c \frac{\partial T}{\partial t} = K\left(\frac{\partial^2 T}{\partial x^2} + \frac{\partial^2 T}{\partial y^2}\right) + Q \tag{4}$$

where ρ is the density (kg m^{-3}), c is the heat capacity (J kg^{-1}K^{-1}), K is the thermal conductivity (J m^{-1}s^{-1} K^{-1}), and Q is the rate of heat generation in the domain (J m^{-3}s^{-1}). In our case, Q is the rate of heat release rate per unit volume during crystallization, which is determined by the growth rate. In our simulation, it can be expressed as

$$Q = \frac{\Delta H_f}{V_m} \cdot \frac{u \cdot ds}{dx \cdot dy} \tag{5}$$

where V_m (m^3 mole^{-1}) is the molar volume of water, ds is the interface length within each mesh grid, and dx and dy are the mesh edge lengths. A standard ADI (Alternate Direction Implicit) scheme is employed here to solve the temperature equation [21].

One of the difficulties of the simulation is to track the moving boundary, which is hard to implement using general numerical meshing schemes. We used the Level Set approach [22] to capture the moving ice front. Several studies [23–25] have demonstrated the applicability of the level set method to simulate liquid crystallization (i.e., the Stefan problem). In this study, our main focus was not on the algorithm itself, but rather on how the simulation can give us useful information to explain the phenomena that Helmuth and Kumpf observed. Therefore, we applied the algorithms proposed in [23] and [26], with modifications necessary to adapt it for our case. More details about the method are discussed in refs. [27] and [28].

The basic idea of the level set method is to construct a level set function, ϕ, to track the position of the interface [22,23]. At any given time t, the value of ϕ at any point is the distance from that point to the interface, positive for water and negative for ice. The interface is then implicitly described by the function $\phi(x, y, t) = 0$, and to track the moving interface, we need to solve for the level set function $\phi(x, y, t)$ in the domain.

The governing equation for evolution of the level set function is

$$\phi_t = -u_c|\nabla\phi| \approx -u_c \tag{6}$$

where u_c is the speed of the contour line in the direction normal to itself and the subscript t indicates a partial derivative with respect to time. The second equality in Eq. (6) reflects the condition that the magnitude of the gradient of ϕ is approximately unity; this is enforced by a reinitialization step [26]. By solving Eq. (6), we obtain ϕ for each time step, so we know the position of the interface. To update the level set function ϕ using Eq. (6), we need to know u_c. At the interface, $u_c = u$ is the ice growth rate given by Eq. (3). To calculate u_c away from the interface, we used the following equation suggested by Adalsteinsson and Sethian [26]:

$$\nabla u_c \cdot \nabla\phi = 0 \tag{7}$$

The gradient of ϕ is normal to the contour lines, so this equation requires that the velocity be uniform (i.e., have zero gradient) normal to the contours. Thus, this method assigns a velocity to all points in the domain such that points on a curve normal to the contour lines will have the same u (see Fig. 5). As shown in [26], this method guarantees that ϕ remains a signed distance function during the propagation. In practice, we start from the interface, where $u_c = u$, then step by step we solve for u_c away from the interface using Eq. (7).

To take into account the Gibbs–Thomson effect on the melting point of the curved ice front, we need the curvature of any point at the

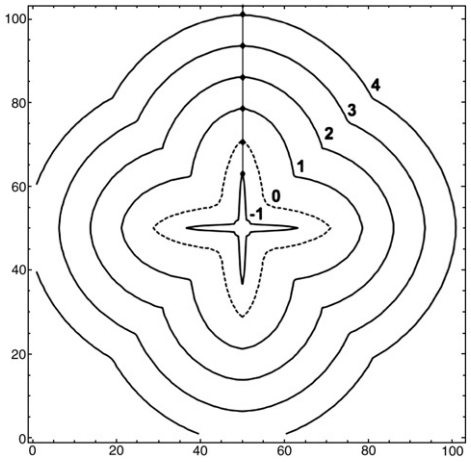

Fig. 5. Schematic of contour lines of $\phi(x, y, t)$, with the crystal/liquid interface ($\phi = 0$) shown dashed. The gradient of ϕ is normal to the contours, and each curve moves away from the interface at the same velocity, u_c. The velocity of the points on the line is found in Eq. (7).

interface. As explained in ref. [29], since ϕ has been constructed to be a signed distance function, the curvature κ can be calculated as

$$\kappa = \nabla\cdot\left(\frac{\nabla\phi}{|\nabla\phi|}\right) = \frac{\phi_y^2\phi_{xx} - 2\phi_x\phi_y\phi_{xy} + \phi_x^2\phi_{yy}}{\left(\phi_x + \phi_y\right)^{3/2}} \tag{8}$$

where the subscripts indicate partial differentials with respect to the spatial variables.

Having set up all the governing equations, we can now outline the numerical steps. Assuming that we know ϕ^n and T^n (i.e., the level set function and temperature at time step n, respectively), the updating algorithm is then as follows:

i) $\phi^n \rightarrow \kappa^n$, curvature of the interface, by Eq. (8)
ii) T^n, $\kappa^n \rightarrow u_c^n$, by Eqs. (1), (3) and (7)
iii) $u_c^n \rightarrow Q^n$, by Eq. (5)
iv) Q^n, $T^n \rightarrow T^{n+1}$, by Eq. (4)
v) ϕ^n,$u_c^n \rightarrow \phi^{n+1}$, by Eq. (6)
vi) If solution not complete, $n \rightarrow n+1$, go to step (i)

To simulate Helmuth's experiment, the domain size was 15×5 cm, with a rectangular mesh with node spacing of 0.05 cm. We used an adaptive time step with the initial step size chosen according to the commonly used stability criterion [30],

$$\Delta t \le \frac{\rho c}{K}\left(\frac{\Delta x}{2}\right)^2 \tag{9}$$

The time step was further adjusted according to the growth rate, u, so that it would take m steps for the ice to cross on one grid:

$$\Delta t \le \frac{1}{m}\frac{\Delta x}{u} \tag{10}$$

where $m = 5$–10. Convergence was studied for the case of a single dendrite using a water domain size of 0.2×0.2 cm, with grid sizes of 0.0005, 0.001, 0.002, 0.004, and 0.008 cm. When the mesh size is smaller than the tip radius of the dendrite, the growth rate quickly converges to a steady value, which is controlled by the rate at which the latent heat is transferred away from the interface. The steady-state rate converges slowly as the mesh is refined, as shown in Section 2.4.

2.2. Simulation versus analytical solution

To test the numerical model, we perform two tests in situations where analytical solutions can be achieved. The first is for ice growth with a planar crystal/liquid interface. If the coordinate system moves with the interface, the temperature of the liquid is described by

$$\frac{\partial T}{\partial t} = \alpha\frac{\partial^2 T}{\partial x^2} + u\frac{\partial T}{\partial x} \tag{11}$$

where $\alpha = K/(c\cdot\rho)$ is the thermal diffusivity ($m^2\ s^{-1}$). The boundary condition is

$$K_C\frac{\partial T_C}{\partial x}|_{x=0} - K_L\frac{\partial T_L}{\partial x}|_{x=0} = \frac{\Delta H_f u \phi_C}{V_C} \tag{12}$$

where $x = 0$ at the crystal/liquid interface, V_C is the molar volume of the crystal, and ϕ_C is the volume fraction of freezable water at the interface. Assuming that the growth rate is constant, the solution of Eq. (11) leads to the following expression for the temperature at the water/ice interface:

$$T_i(t) = T_\infty + \lambda\left[\sqrt{\frac{t}{\pi\cdot\tau}}\exp\left(-\frac{t}{4\tau}\right) - \frac{t}{2\tau} + \left(1 + \frac{t}{2\tau}\right)erf\left(\sqrt{\frac{t}{4\tau}}\right)\right] \tag{13}$$

where T_∞ = temperature far from the interface, the characteristic time is $\tau = \alpha/u^2$, and the characteristic temperature is $\lambda = \Delta H_f/(V_C\cdot c\cdot\rho)$. This solution predicts that the interface temperature will rise rapidly, because the latent heat is being generated at a constant rate, but diffusion removes it at a rate that decreases with the square root of time.

On the other hand, if the growth rate decreases as $u = u_0/t^{1/2}$, then the temperature of the interface remains constant. In this case, the solution of Eq. (11) is

$$T(x,t) = T_\infty + \sqrt{\pi}\lambda\mu\exp\left(\mu^2\right)\left[1 - erf\left(\mu + \frac{x}{2\sqrt{\alpha t}}\right)\right] \tag{14}$$

where $\mu = u_0/\alpha^{1/2}$, so the temperature of the interface, $T_i = T(0,t)$, is

$$T_i = T_\infty + \lambda\mu\sqrt{\pi}\exp\left(\mu^2\right)erfc(\mu) \tag{15}$$

The numerical results agree well with the theoretical solutions, as shown in Fig. 6.

2.3. Simulation of Helmuth's experiment

To simulate Helmuth's experiment, we implemented the model within a 2-D rectangular domain (3 cm by 15 cm). If we were investigating a property that depended on pore connectivity, such as the pore pressure, it would be necessary to use a 3-D model. However, the goal of the calculation is to evaluate the pattern of growth, which results from the temperature distribution, so we can get a semi-quantitative approximation from a 2-D simulation. The heat capacity and thermal conductivity of materials used in our simulation are as follows [31]: $c_{water} = 4.19\ J\ g^{-1}K^{-1}$, $c_{ice} = 1.97\ J\ g^{-1}K^{-1}$, $c_{concrete} = 0.96\ J\ g^{-1}\ K^{-1}$, $K_{water} = 0.0058\ J\ s^{-1}\ cm^{-1}\ K^{-1}$, $K_{ice} = 0.022\ J\ s^{-1}\ cm^{-1}\ K^{-1}$, $K_{concrete} = 0.017\ J\ s^{-1}\ cm^{-1}\ K^{-1}$. The heat of fusion of water is $\Delta H_f/V_C = 334\ J/cm^3$. We assume that the freezable water content of the sample is $\phi_C = 0.1$ by volume, about half of which freezes into dendrites. This ice content is similar to that measured in a mortar with w/c = 0.55, where the ice content at −5 °C was about 3% of the volume of the sample [4]. The initial temperature of the sample is −5 °C and the bath temperature is −7 °C. The freezing is initiated at a point on one of the short edges of the sample. Fig. 7 shows the simulation results.

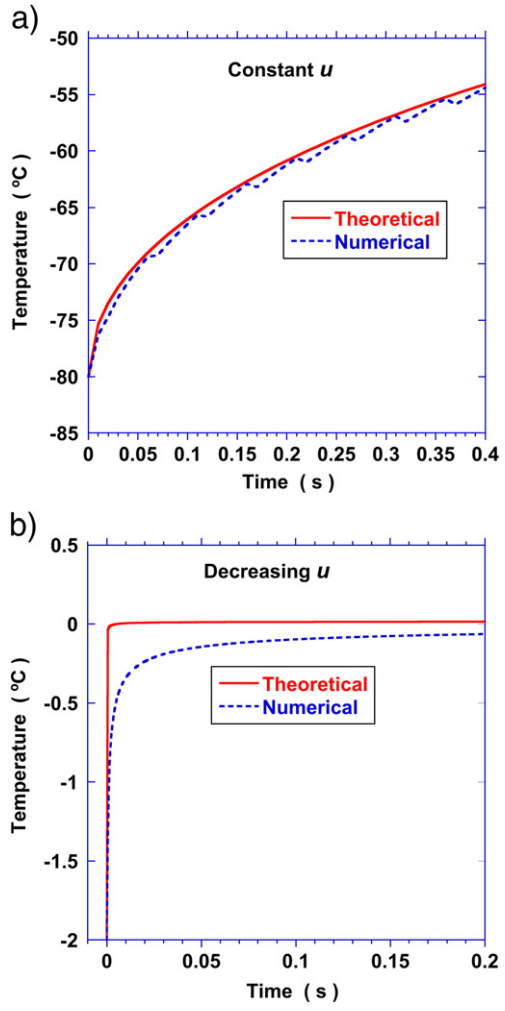

Fig. 6. Interfacial temperature of flat crystal growing at: a) u = constant and b) $u = u_0/t^{1/2}$. Simulations quickly approach the theoretical values given by Eqs. (13) and (15).

A striking prediction of the simulation is that the ice grows in the form of dendrites. When the volume fraction of water is ≥0.1 in the simulation, the pattern of growth is very similar to that in Fig. 7a; at much lower water contents, the scale of the dendrites becomes much finer. The narrow shape of the tip allows heat to be shed more quickly, which allows faster growth. This is consistent with the measurements by Helmuth [13], Kumpf [14], and the present study, which show that ice grows at a constant rate in cement paste, which is not possible under heat-flow control, except when dendrites are present.

In Helmuth's experiment, the sample remained immersed in the kerosene bath during crystallization. To simulate that situation, the boundary of the sample was held at the temperature of the bath. As a result, the calculation predicts that ice grows rapidly along the cold surface. Indeed, Fig. 7a shows that, for most locations inside the block, ice arrives first from the sides, rather than from the end where freezing was initiated. If we mark the positions of the thermocouples in the sample and record their temperature change versus time, as Helmuth did in his experiments, we are able to reproduce the experimental observations: the growth rate is fast, and the temperature jumps of the thermocouples do not occur at uniform intervals (Fig. 7b). The simulations reveal that both of these features are artifacts resulting from rapid growth of ice along the surface, followed by dendritic growth inward.

This pattern of growth (i.e., the occurrence of dendrites, the growth rate of a single dendrite, and the rapid growth along the cold edge) is not affected by the point of nucleation that we choose. The sequence of contacts of the ice with the thermocouples changes only slightly from run to run, as is true of the experiments. For example, in Fig. 7a, different initiating positions might cause thermocouples 5 and 6 to respond together, instead of 4 and 5, or there might be no simultaneous responses. In any case, the behavior of the simulations is consistent with the experiments, in that the rate of growth is high and the triggering of the thermocouples is slightly erratic.

Another simulation was run in which the boundary was insulated (i.e., the flux across the surface was set to zero) to prevent fast growth along the edge. In this case, as shown in Fig. 8a, ice grows dendritically from one end to another, and the temperature jump pattern of the thermocouples is more uniform (Fig. 8b). As shown in Fig. 9, the true growth rate from the insulated boundary condition is ~1/3 of the apparent growth rate found with the cold boundary condition.

2.4. Dendritic ice growth and the simulation

Dendritic crystal growth has been studied intensively for decades, with the goal of predicting the dependences of tip radius, growth rate, and branch position on the degree of undercooling and the material properties. A good review can be found in ref. [32]. Among the many theories that have been proposed, several deserve special mention. Ivantsov [33] was the first to obtain a solution for the steady-state growth of a dendrite under heat-flow control. By assuming the dendrite surface to be a paraboloid of revolution and isothermal, he showed that the product of the radius of curvature of the tip, R, and the growth rate, u, is constant at a given underdooling, $\Delta T = T_{m\_} T$. The implicit solution is

$$S_t = P_e \cdot e^{Pe} \cdot \int_{Pe}^{\infty} \frac{\exp(-z)}{z} dz \tag{16}$$

where S_t is the dimensionless undercooling, or Stefan number, defined as

$$S_t = \frac{\Delta T \cdot c \cdot V_m \cdot \rho}{\Delta H_f} \tag{17}$$

and P_e is the dimensionless Peclet number defined as

$$P_e = \frac{uR}{2\alpha} \tag{18}$$

Horvay and Cahn [34] extended the analysis to elliptical paraboloids, including the 2-D case (the parabolic platelet), where Eq. (16) becomes

$$S_t = \sqrt{\pi \cdot P_e} \cdot e^{Pe} \cdot erfc\left(\sqrt{P_e}\right) \tag{19}$$

Our purpose here is to see how our simulation compares to Eq. (19). For this purpose, we simulate the growth of a single dendrite, so that the tip location is easy to track. As shown in Fig. 10a, when the mesh size is <R, the growth rate quickly converges to a steady value, which is controlled by the rate at which the latent heat is transferred away from the interface. The steady-state rate converges slowly as the mesh is refined, as shown in Fig. 10b. It is more difficult to find R from the simulation than u, as the radius of a parabolic curve is not constant in the region close to the tip (e.g., the curvature of a parabolic curve at a distance R from the tip is about 1/3 of the curvature at the tip). Fig. 10c shows the shape of the tip, defined by the locus of $\phi = 0$, compared to the shape found from Eq. (19) using u from the simulation, and the curvature calculated from Eq. (8). The comparison is quite satisfactory.

Although our simulation agrees well with the Horvay–Cahn theory, it cannot be used for quantitative prediction of u and R. The details are beyond the scope of this study, but a brief justification is presented as follows. The theories from Ivantsov and Horvay–Cahn

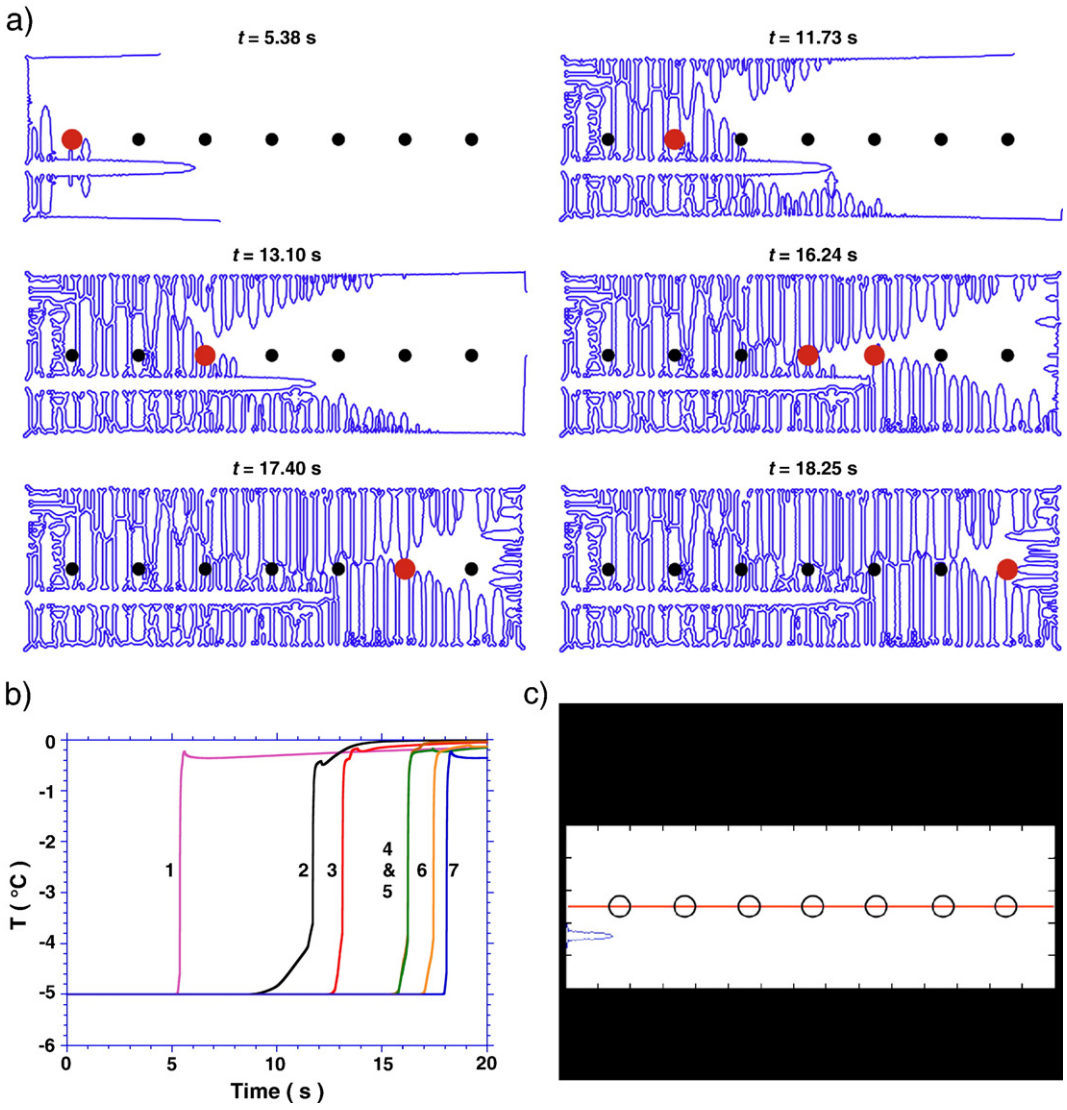

Fig. 7. a) Simulation of dendritic growth in cement paste with cold boundary condition; the dark boundary around each dendrite represents the locus of $\phi = 0$. The dots along the axis of the sample are thermocouple locations, and the shaded dot is the one that reports a jump in temperature at the indicated time. Except for the first two, the thermocouples are engulfed by dendrites growing in from the edge. b) Calculated temperature jumps of thermocouples. c) Animation of dendritic growth in cement paste with cold boundary condition.

represent important steps in theoretical analysis of dendritic growth, but they are not deterministic, because they only provide the product of u and R. To determine u and R, an additional rule (i.e., the velocity selection mechanism) must be applied. Several mechanisms have been proposed, among which, the marginal stability theory [18] and the microscopic solvability theory [35] are the most widely studied. The marginal stability theory proposed by Langer and Muller-Krumbhaar [18] agrees best with experimental data [32]. It is based on the assumption that the radius of the tip is equal to the critical wavelength for stability of a planar interface. Although this is physically plausible, there is no fundamental basis for it, and it is difficult to implement the theory in a numerical simulation. In particular, we do not impose the tip curvature in our level set simulations, and we find that it does not agree with the prediction of marginal stability theory. The microscopic solvability, on the other hand, has been used extensively in numerical studies [24,25,36]. Although the results of those simulations agree well with the analytical theory, as pointed out in [32], the microscopic solvability theory itself does not correctly predict the rate of dendritic crystal growth observed experimentally. In our model, we require the interface velocity to obey Eq. (3), and solve the heat equation to get the pattern of ice growth, so u and R are determined by the interplay of heat flow and capillary effects. The results are not predictive, however, because our heat-flow analysis is 2-dimensional, whereas Eq. (3) was obtained from 3-dimensional experiments, and the growth rates in 2 and 3 dimensions are predicted to be very different [34]. Therefore, in this study, we use the simulation only to obtain qualitative information about the ice growth pattern in Helmuth's experiment. This has enabled us to reinterpret the experiment, as described in next section.

3. Experimental verification

3.1. Procedure

As the simulation offered a possible explanation for the rapid growth indicated by Helmuth's experiment, a revised version of the experiment was conducted to verify the findings. Samples of ordinary cement paste of both Type I and Class H were prepared with w/c = 0.45–0.65, then cured in lime-saturated water for about two weeks. The samples were in the form of rectangular prisms approximately $22 \times 7 \times 5$ cm with thermocouples embedded along

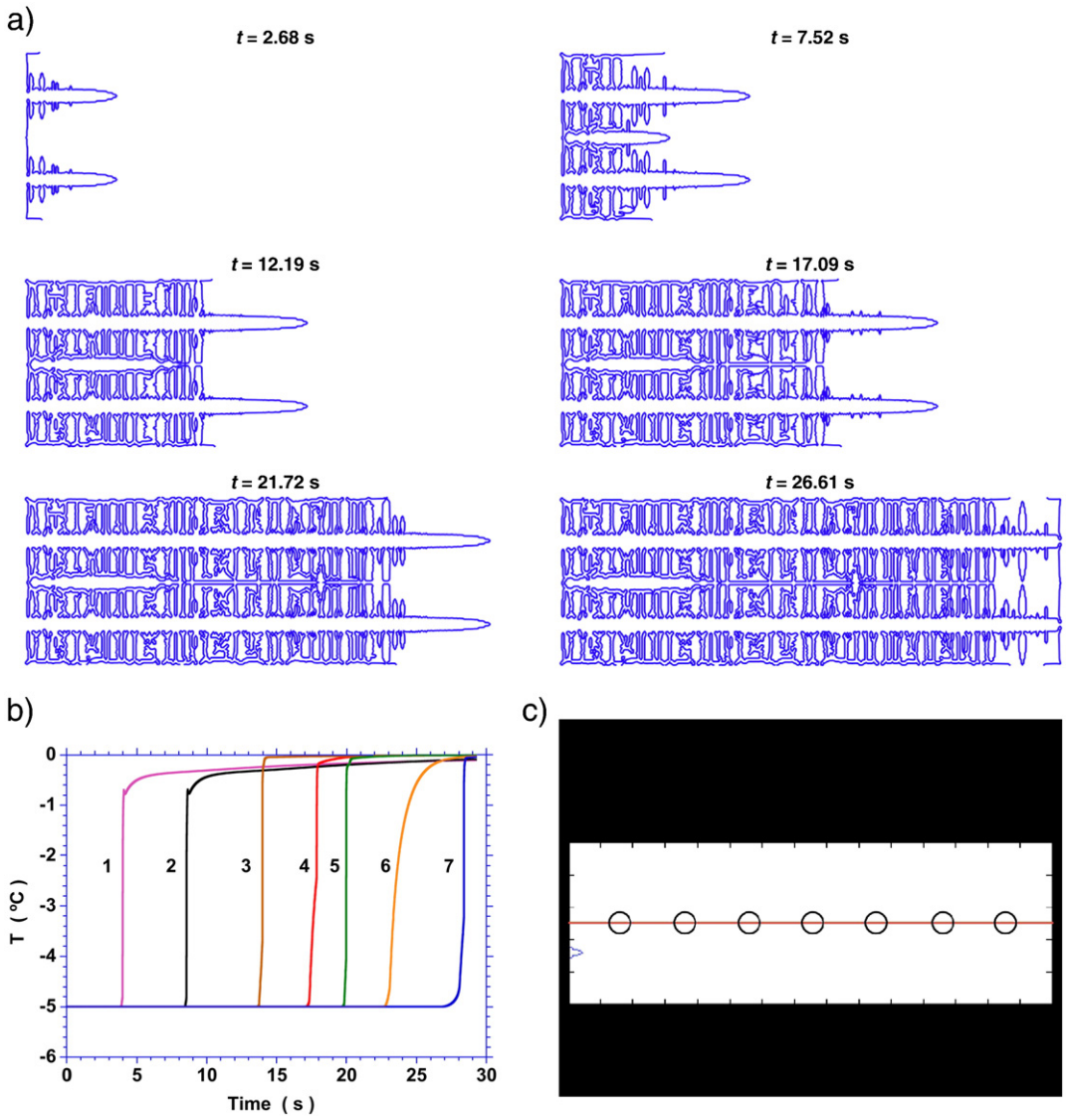

Fig. 8. a) Simulation for insulated boundary condition; the dark boundary around each dendrite represents the locus of $\phi = 0$. b) Temperature jump of thermocouples. c) Animation of dendritic growth in cement paste with insulated boundary condition.

the mid-plane every 2.7 cm. The cement powder was mixed in a kitchen mixer for 1 min before water was added; the mixture was then mixed for 2 more minutes and poured into the molds. The thermocouples were inserted into the molds immediately. After 24 h the samples were demolded and cured in lime-saturated water for about two weeks. During the test, the paste blocks were immersed in a kerosene bath at temperatures between about −2.5 and −5 °C, and freezing was nucleated by touching the end of the block with ice. As in the simulation, two different boundary conditions were applied: a cold surface and an insulated surface. The cold surface case was the same as Helmuth' procedure, while the insulated surface condition was achieved as follows. After the sample temperature equilibrated with the bath temperature, instead of leaving it in the bath, the sample was lifted out and touched with ice. In this case, the surface of the sample was insulated by room air, so that the heat could not be transferred away quickly.

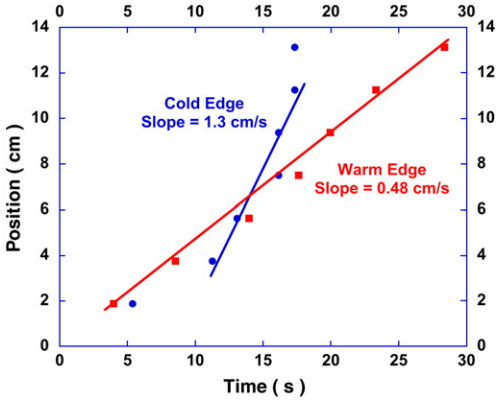

Fig. 9. Comparison of ice growth rate of cold boundary (Cold Edge, round symbols) and insulated boundary (Warm Edge, square symbols) conditions from simulation.

To study the nucleation temperature of cement paste, cylindrical samples, 3.8 cm (D) × 6.4 cm (H), both with and without air voids, were prepared. The mixing procedure was the same as above, except that only Type I and w/c = 0.45 were used. The air entrainment agent (Sika Air) was added to the water before mixing at a concentration sufficient to produce 6% air. Each sample had one thermocouple embedded in the center. During the test, the samples were immersed in the kerosene bath and cooled to −12 °C at the rate of ~0.3 °C/min.

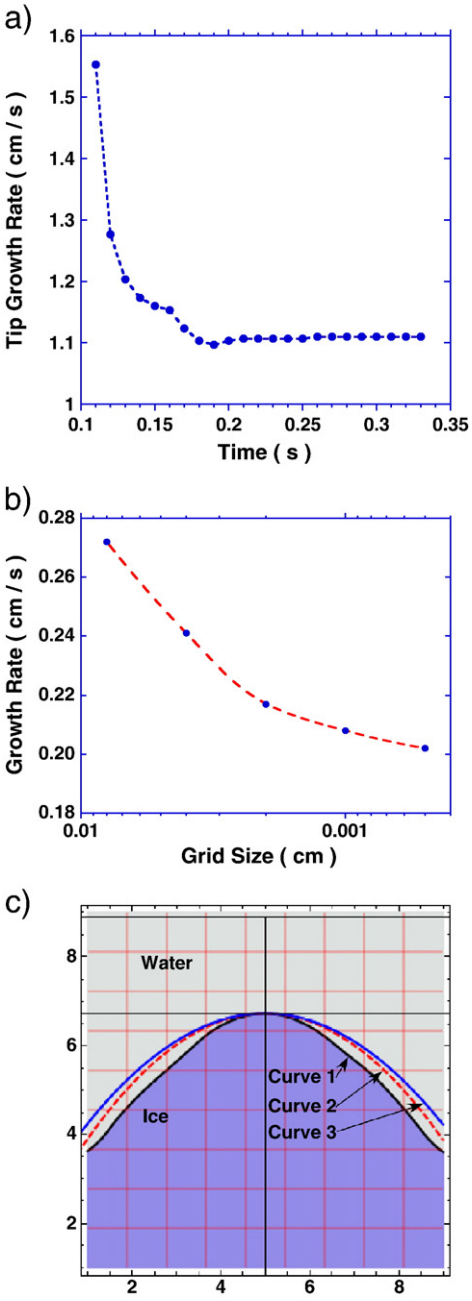

Fig. 10. a) Growth rate is fast at the beginning, then converges to a steady rate as the temperature field stabilizes; b) growth rate versus mesh size; c) tip shape of dendrite from the level set function $\phi(x,y)=0$ (Curve 1), from Eq. (19) using the growth rate u from the simulation (Curve 2), and calculated from Eq. (8).

The surface temperature of the sample was recorded by a thermocouple put directly in the bath, while the internal temperature was recorded through the embedded thermocouple.

3.2. Results

The results, which agreed well with the findings from the simulation, as shown in Fig. 11. For the cold surface boundary condition, the thermocouples responded in exactly the same way that Helmuth found, reflecting a fast growth rate along the edge. In contrast, with the insulated surface boundary condition, the thermocouples responded one after another much more uniformly, reflecting the true and much slower ice growth rate. This is clearly seen from Fig. 12, which shows that the ice growth rate in the sample with the cold surface is ~0.3–0.7 cm/s, while that in the sample with the insulated surface sample is 0.19 cm/s.

4. Discussion

Both the simulations and experiments suggest that ice growth in supercooled cement paste is in the form of dendrites. This form of growth is favored, because the shape of the tip allows the heat to disperse more quickly, resulting in faster ice growth. Indeed, dendrites are expected when ice forms in supercooled bulk water; however, we are not aware of any other studies of dendritic growth within a porous host. As dendrites penetrate through the sample, the freezing rate decreases until the rates of heat generation and diffusion from the crystal/liquid interface are in balance. The temperature between dendrite branches increases toward the melting point of the liquid in the pores. This temperature distribution is schematically illustrated in Fig. 13. Helmuth first suggested that the final temperature of the thermocouples is related to the pore size due to the Gibbs–Thomson effect, which is expressed by Eq. (1). Kumpf [14] systematically investigated the relationship between the two, using mercury porosimetry to measure the pore size of the paste, and his result supported Helmuth's argument.

One thing that is not certain is the size of the dendrites in the sample. Helmuth mentioned possible dendritic ice growth inside his cement paste [13], but did not discuss their structure. We conclude that dendrites cannot exist within the mesopores, because Eq. (1) indicates that the high curvature of such a crystal would push its melting point far below the range at which freezing occurs in the paste. Our speculation is that the size of a dendrite is much larger than that of the pores, so each branch actually includes a cluster of pores. This idea has not been verified by direct observation. However, in ref. [37], Abellan performed numerical simulations using the phase-field method to study crystallization in pores, and the results clearly

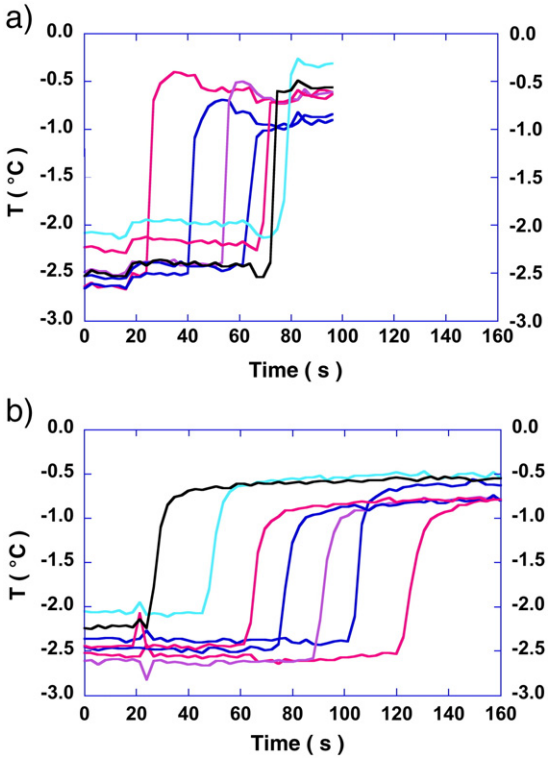

Fig. 11. Revised Helmuth experiments: measured temperature jumps in samples with (a) Cold boundary and (b) Insulated boundary. Bath temperature = −2.5 °C, internal temperature after jump ≈ −0.7 °C.

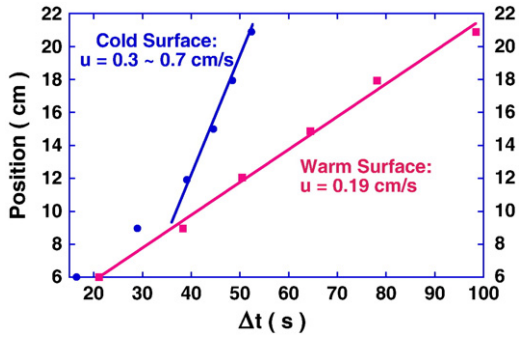

Fig. 12. Growth rate found from revised Helmuth experiments as shown in Fig. 11, where bath temperature is −2.5 °C.

supported the possibility that each dendrite branch incorporates many pores inside, as shown in Fig. 14.

Helmuth interpreted his measured growth rates to be the internal growth rate of ice within the paste. However, our revised experiment, where freezing occurs outside of the bath, shows that the actual growth rate is ~1/3 of the apparent rate found when the sample is immersed in the cooling bath. This explains the contradictory finding discussed in the Introduction, which is that Helmuth measured "heat-flow controlled" growth rates that were comparable to interface kinetics-controlled growth rates measured by Hillig and Turnbull. The reason is that the measured growth rate in the submerged sample was actually the growth rate on the cold surface, where the heat does not accumulate and the growth is actually controlled by interface kinetics, so it has to be comparable to the growth rate measured by Hillig and Turnbull.

The ice growth rate and pattern are important for the resultant stress in a concrete body. It was pointed out in ref. [13] that undercooling is very common in nature. Thus, it is highly possible that dendritic ice growth occurs when concrete freezes in the field. When ice grows, it pushes the adjacent water away, due to the volume change, and generates pressure [2]. If the ice grows slowly and the pores are not blocked, the pressure can be relieved by water flow through the pore system to external surfaces or interior voids; however, if the ice grows too fast, the pressure can be sufficient to damage concrete. What constitutes "too fast" depends on the permeability of the paste and the distance between voids, as shown by Powers [2]. In some situations, such as the Helmuth experiment, the ice forms at the surfaces of the sample first. This could lead to a bad situation, if the water inside the sample becomes entrapped by ice-blocked pores, so that it cannot get away when the freezing front moves inwards. Freezing of trapped water can cause severe damage in highly saturated cement paste [38].

The growth rate of ice depends strongly on the degree of undercooling, according to Eq. (3). Thus, if we can encourage nucleation at a relatively high temperature, we can reduce the

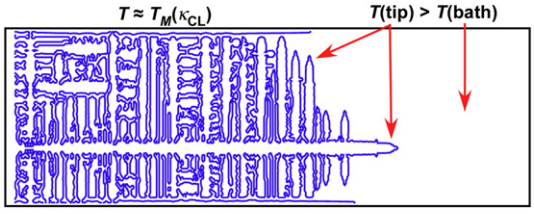

Fig. 13. Schematic illustration of dendrites indicating that the growing tips remain at a temperature below the melting point, but above the temperature of the bath. The rate of growth of the tip is controlled by its temperature, according to Eq. (3), and its temperature is controlled by the rate of heat flow into the bath. Far behind the tip, the temperature between the dendrites reaches the melting point, which is related to the pore size by Eq. (1); the liquid in that region gradually freezes as the heat diffuses away.

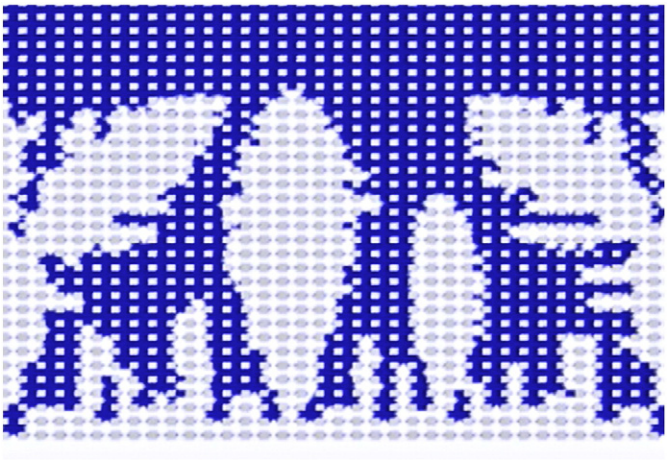

Fig. 14. Pore-scale simulation of crystallization in pores by the phase-field method, where the dark regions are liquid and the gray squares represent the solid phase. Growth of dendrites (white) occurs on a scale much larger than the pore diameter. Figure from Abellan [37].

magnitude of the hydraulic pressure from the ice growth. In the absence of air entrainment, avoiding large undercoolings is essential, so introducing a nucleating agent into the paste might be helpful. Even in the case of air-entertained concrete, stimulating nucleation could help, but only if the nucleating agent is in the voids, rather than in the paste. It was shown in [4] that air voids protect concrete in two ways. First, they reduce hydraulic pressure by providing room for water to expand at the beginning of the freezing process, when ice nucleates in the mesopores. Second, once ice has formed in the air voids, they provide space for the unconfined growth of that ice, which sucks water from adjacent mesopores, generating negative pressure. If the undercooling is too large when nucleation first occurs, the concrete could be damaged by the hydraulic pressure from the initial burst of ice growth, in spite of the voids. This might be avoided by introducing nucleating agents into the air voids, so that ice forms inside them before it nucleates in the mesopores [39]. However, if too much ice is created in the mesopores, it could offset the benefit of the negative pore pressure generated by the ice in the voids, so dispersing nucleating agents in an air-entrained paste would probably be counter-productive.

The results in Fig. 15 show that the presence of air voids does not promote nucleation. The experiment was done as follows. Samples of ordinary cement paste (with and without air voids) were cast with thermocouples embedded in them. The samples were then put into the cooling bath and the thermocouples were monitored as the samples cooled. The nucleation event was indicated by the sudden temperature change due to the heat released as pore water froze, and it reproducibly occurred at the same temperature for samples with and without entrained air. A similar result was obtained in ref. [4] for much smaller samples. The fact that nuclei do not form preferentially in the voids means that pressure pulses are inevitable, because nucleation occurs in the mesopores of the paste. This could contribute to fatigue from repeated freeze/thaw cycles. For water in air voids to nucleate at higher temperatures, and thereby create suction in the pore liquid that offsets the pressure exerted by crystals nucleated in mesopores, it will apparently be necessary to introduce nucleating agents into the voids [39].

5. Conclusions

Helmuth concluded correctly that ice grows in cement paste under heat-flow control and that the internal temperature rises to the melting point given by the Gibbs–Thomson equation [13]. However, the rates that he measured agree with the values obtained when

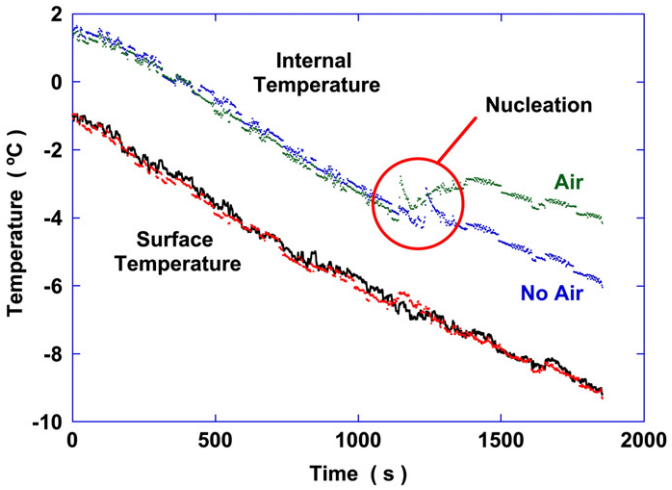

Fig. 15. Samples with and without air entraining agent (AEA) freeze at almost the same temperature. The freezing is indicated by the temperature jump at ~1200 s (Nucleation), and the magnitude of the change reflects the amount of water that freezes. It is apparent that more ice forms in the sample with AEA.

growth is controlled by interface attachment kinetics [16]. Our numerical simulations and experiments explain the contradiction: Helmuth measured the fast growth rate along the cold sample surface, which is in fact interface kinetics-controlled growth at the temperature of the bath. We show that the ice in cement paste grows in the form of dendrites, and the temperature between the dendrite branches is at the melting point of the liquid in the pores. A simple modification of Helmuth's experiment (*viz*., lifting the sample out of the cold bath before nucleation occurs) allows measurement of the true rate of growth of the dendrites. By understanding the rate and pattern of ice growth, it will be possible to develop better models of the stress development during freezing.

Acknowledgment

This work was supported by NSF grant CMS-0509986.

References

[1] J. Marchand, R. Pleau, R. Gagné, Deterioration of concrete due to freezing and thawing, in: J. Skalny, S. Mindess (Eds.), Materials Science of Concrete IV, Am. Ceram. Soc., Westerville, OH, 1995, pp. 283–354.
[2] T.C. Powers, The air requirement of frost-resistant concrete, Proc. Highway Res. Board 29 (1949) 184–211.
[3] J.J. Beaudoin, C. MacInnis, The mechanism of frost damage in hardened cement paste, Cem. Concr. Res. 4 (1974) 139–147.
[4] Z. Sun and G.W. Scherer, "Effect of Air Voids on Salt Scaling", Cement & Concrete Research 40 (2010) 260–270.
[5] T.C. Powers, R.A. Helmuth, Theory of volume changes in hardened Portland-cement paste during freezing, Proc. Highway Res. Board 32 (1953) 285–297.
[6] H.F.W. Taylor, Cement Chemistry, 2nd ed.Thomas Telford, London, 1997.
[7] R. Defay, I. Prigogine, Surface Tension and Adsorption, Wiley, New York, 1966.
[8] G.W. Scherer, J.J. Valenza II, Mechanisms of frost damage, in: J. Skalny, F. Young (Eds.), Materials Science of Concrete, vol. VII, American Ceramic Society, 2005, pp. 209–246.
[9] M. Brun, A. Lallemand, J.F. Quinson, C. Eyraud, A new method for the simultaneous determination of the size and the shape of pores: the thermoporometry, Thermochim. Acta 21 (1977) 59–88.
[10] Z. Sun and G.W. Scherer, "Pore Size and Shape in Mortar by thermoporometry", Cem. Concr. Res. 40 (2010) 740–751.
[11] O. Coussy, P.J.M. Monteiro, Poroelastic model for concrete exposed to freezing temperatures, Cem. Concr. Res. 38 (2008) 40–48.
[12] M. Pigeon, R. Pleau, Durability of Concrete in Cold Climates, E & FN Spon, London, 1995.
[13] R.A. Helmuth, Capillary size restrictions on ice formation in hardened Portland cement pastes, Proc. 4th Int. Cong. Chemistry of Cement, NBS Monog. 43, Vol. II, National Bureau of Standards, Washington, D.C, 1962, pp. 855–869.
[14] D. Kumpf, "The relationship between pore structure and ice growth rate in hardened Portland cement paste", Senior thesis, Dept. Civil & Env. Eng., Princeton University, 2004
[15] Z. Sun, D. Kumpf, G.W. Scherer, "Kinetics of ice growth in concrete", paper W4-07.1, in: J.J. Beaudoin, J.M. Makar, L. Raki (Eds.), Proc. 12th Int. Cong. Cement Chemistry, National Research Council of Canada, Montreal, Canada, ISBN: 978-0-660-19695-4, 2007.
[16] W.B. Hillig, D. Turnbull, Theory of crystal growth in undercooled pure liquids, J. Chem. Phys. 24 (4) (1956) 914.
[17] K.A. Jackson, D.R. Uhlmann, J.D. Hunt, On the nature of crystal growth from the melt, J. Cryst. Growth 1 (1967) 1–36.
[18] J.S. Langer, H. Müller-Krumbhaar, Theory of dendritic growth — I. Elements of a stability analysis, Acta Metall. 26 (1978) 1681–1687.
[19] J.S. Langer, Instabilities and pattern formation in crystal growth, Rev. Mod. Phys. 52 (1) (1980) 1–28.
[20] A.A. Shibkov, M.A. Zheltov, A.A. Korolev, A.A. Kazakov, A.A. Leonov, Crossover from diffusion-limited to kinetics-limited growth of ice crystals, J. Cryst. Growth 285 (2005) 215–227.
[21] D.W. Peaceman, H.H. Rachford Jr., The numerical solution of parabolic and elliptic differential equations, J. Soc. Ind. Appl. Math. 3 (1955) 28–41.
[22] S. Osher, J. Sethian, Front propagating with curvature-dependent speed: algorithms based on Hamilton–Jacobi formulation, J. Comput. Phys. 79 (1988) 12–49.
[23] S. Chen, B. Marriman, S. Osher, P. Smereka, A simple level set method for sloving steven problems, J. Comp. Phys. 135 (1997) 8–29.
[24] F. Gibou, R. Fedkiw, R. Caflisch, S. Osher, A level set approach for the numerical simulation of dendritic growth, J. Sci. Comput. Arch. 19 (1–3) (2003) 183–199.
[25] Y.-T. Kim, N. Goldenfeld, J. Dantzig, Computation of dendritic microstructures using a level set method, Phys. Rev. E 62 (2) (2000) 2471–2474.
[26] D. Adalsteinsson, J.A. Sethian, The fast construction of extension velocities in level set methods, J. Comput. Phys. 148 (1999) 2–22.
[27] J.A. Sethian, Level Set Methods and Fast Marching Methods: Evolving Interfaces in Computational Geometry, Fluid Mechanics, Computer Vision, and Materials Science, 2nd ed.Cambridge University Press, Cambridge, 1999.
[28] S.J. Osher, R.P. Fedkiw, Level Set Methods and Dynamic Implicit Surfaces, Springer, Secaucus, NJ, 2003.
[29] J.A. Sethianand, J.D. Strain, Crystal growth and dendritic solidification, J. Comp. Phys. 98 (2) (1992) 231–253.
[30] S. Chapra, R. Canale, Numerical Methods for Engineers: with Software and Programming Applications, 4th editionMcGraw-Hill, New York, 2001.
[31] The Engineering ToolBox, http://www.engineeringtoolbox.com.
[32] M.E. Glicksman, S.P. Marsh, The dendrite, in: D.T.J. Hurle (Ed.), Handbook of Crystal Growth, vol. 1, Elsevier, Amsterdam, 1993, pp. 1075–1122.
[33] G.P. Ivantsov, Temperature field around spherical cylindrical and needle-shaped crystals which grow in supercooled melt, Dokl. Akad. Nauk SSSR 58 (1947) 567–569.
[34] G. Horvay, J.W. Cahn, Dendritic and spheroidal growth, Acta Metall. 9 (1961) 695–705.
[35] A. Barbieri, J. Langer, Predictions of dendritic growth rates in the linearized solvability theory, Phys. Rev. A 39 (1989) 5314–5325.
[36] A. Karma, Phase-field formulation for quantitative modeling of alloy solidification, Phys. Rev. Lett. 87 (2001) 11.
[37] O. Abellan, "Transport in Porous Matrices: An Application of the Phase Field Method", MSE Thesis, Dept. Civil & Env. Eng., Princeton University 2007.
[38] S. Chatterji, Aspects of the freezing process in a porous material–water system. Part 1. Freezing and the properties of water and ice, Cem. Concr. Res. 29 (1999) 627–630.
[39] G.W. Scherer, J. Chen, and J. Valenza, "Method of protecting concrete from freeze damage", U.S. Pat 6, 485, 560 (Nov. 26, 2002).